Int. J. Appl. Ceram. Technol., 10 [3] 484–491 (2013)
DOI:10.1111/j.1744-7402.2012.02752.x

International Journal of
Applied Ceramic TECHNOLOGY
Ceramic Product Development and Commercialization

Laser Machining and Functional Applications of Glass-Ceramic Materials

Daniel Sola*

Departamento de Física Aplicada I, Centro de Física de Materiales, Universidad del País Vasco-CSIC, Bilbao E-48.013, Spain

Jose I. Peña

Departamento de Ciencia y Tecnología de Materiales y Fluidos, Instituto de Ciencia de Materiales de Aragón, Universidad de Zaragoza-CSIC, Zaragoza E-50.018, Spain

In this work a study of glass-ceramic laser machining and some functional applications are presented. Firstly, both the effect produced by the machining method as well as how the modification of the reference position influence the machining results have been studied. Secondly, blind holes and special shape cross-section blind holes have been created for functional purposes. A Q-switched Nd:YAG laser at its fundamental wavelength of 1064 nm with pulse-widths in the nanosecond range has been used. Morphology, depth, and volume obtained by machining grooves have been studied. The variation in the ablation yield when the position of the surface to be machined is modified has also been studied. The composition and microstructure of the machined areas have been described and discussed and thermal tests have been performed to check if the objectives of the functional applications have been achieved.

Introduction

Laser processing is of great interest in the field of optics, electronics, microelectronics, aerospace, and medicine. This technique is cost effective compared to traditional methods and it may be applied to a wide range of substrates, such as metals, ceramics, and semiconductors.[1] In the field of materials processing by laser, several methods, such as laser machining, micromachining, marking, drilling, and pulsed laser deposition, have been developed in the last two decades.[2,3] Laser processing has been incorporated in

*daniel_sola@ehu.es

industry over the last few decades. Reduction in production costs, staff, and maintenance savings as well as in tool wearing, make laser processing the most suitable working tool for machining hard and brittle materials.

The appearance of techniques for generating short and ultra short laser pulses, ranging from tens of nanoseconds to a few femtoseconds without variation of other parameters such as pulse energy or the working frequency, have allowed the availability of more powerful systems, with power densities that can reach TW/cm^2. These laser systems, with better features and lower prices, offer a high-speed/high-quality tool for laser machining, which is of great interest in both basic and applied research for scientific and technological purposes.[3,4]

However, the foundations of the mechanisms involved in laser ablation are far from being well established. It is known that laser ablation depends on laser wavelength, optical features of laser beam, pulse-width regime, and optical-thermal-mechanical properties of the substrate. Some theoretical descriptions have been developed by many authors to generalize the stages of the ablation process.[4–19]

Glass and glass ceramic substrates are commonly used in a variety of applications such as lasing systems, opto-informatic devices, micro-optical components, mirrors and waveguides, the optical properties of which are of great interest.[20–24]

In this article, firstly, the effect produced by the machining method and how the modification in the reference position influences the morphology of the geometrical parameters, that is, the ablated depth, the machined diameter and the removed volume, as well the ablation yield have been showed. Afterward, these results have been applied to machine the glass-ceramic substrate for some functional purposes.

Experimental Procedure

Laser Processing

A commercial diode-pumped Nd:YAG laser has been used in this work (E-Line 20, Rofin-Sinar, Hamburg, Germany). The laser system operates at its fundamental wavelength of 1064 nm with a maximum mean power of 11 watts, in a Gaussian beam mode TEM_{00} with a beam quality factor $M^2 < 1.3$. The opto-acoustical Q-Switch commutator controls the cavity output in continuous and in pulsed mode, generating pulses as short as 8 ns in a frequency range of 1–40 kHz.

The beam is deflected by using a programmable galvanometer scanner controlled by CAD software, making a bidirectional movement, in such a way that any predefined pattern and processing procedure can be performed. The machining process is controlled by the diodes pump current I (in relation to peak power), pulse frequency f, linear speed V_L, and distance between adjacent lines Δ. The system is equipped with a beam expansor 5× before the galvanometric mirrors and a convex lens with focal length F of 100 mm. Thus, using the Eq.1:

$$D_{bw} = \frac{4F M^2 \lambda}{\pi D_0} \quad (1)$$

$$R = \left(\frac{\pi D_{bw}^2}{4 M^2 \lambda}\right) \quad (2)$$

where D_0 is the diameter of the laser beam before the optical lens, the diameter at the focal point D_{bw}, and the Rayleigh range R for this system are, approximately, 13 and 96 μm, respectively.

The equipment incorporates a double mirror-revolving system that controls the incidence angle. So, any special shape cross-section blind holes can be created.

Sheets of glass-ceramic substrate (Ceran Suprema®, Schott, North America, Duryea, PA) were used the properties of which are shown in Table I.

In Fig. 1, a sketch of the laser processing is shown. The sample is machined above and below the focal point, varying the reference position around it. The sign convention taken is: negative when the sample is moved upward and positive when it is moved downward.

The laser processing was carried out by modifying the reference distance and using machining grooves with dimensions 2 × 0.3 mm length × width. Laser pulses

Table I. Properties of the Glass-Ceramic Substrate

Density (g/cm^3)	2.5*
Bending strength (MPa)	110*
Hardness vickers	800
Thermal conductivity (W/mK)	1.7 *
Thermal diffusivity (m^2/s × 10^{-6})	0.85†
Melting temperature (ºK)	1498*
Diffuse reflectance (1064 nm)	0,93
Optical absorption $\alpha\vert_{1064\ nm}$ (per cm)	3.52
Absorption length $L_\alpha = \alpha^{-1}\vert_{1064\ nm}$ (cm)	0.28
Thermal diffusion length $L_{th}\vert_{10\ ns}$ (μm)	0.18

*Schott technical data.
†Meassure carried out at the Instituto de Cerámica y Vidrio.

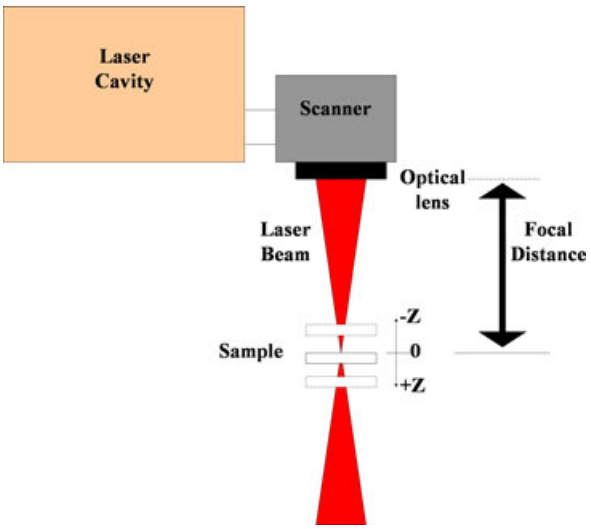

Fig. 1. Sketch of the laser processing.

of 2.7 and 2.45 mJ of energy with peak powers of 300 and 260 kW were used for frequencies of 1, 2 kHz, respectively. A scanning speed of 4 mm/s with a distance between adjacent lines of 10 μm was also used. To attain reliable results, nine samples were machined in each case.

Characterization Techniques

The microstructure and composition have been determined by means of scanning electron microscopy SEM (JSM6400, JEOL, Tokyo, Japan) with EDX analysis. Mechanical characterization was determined by using a micro hardness tester (MXT-70, Matsuzama Seiki, Tokyo, Japan) and an Instron 5565 testing machine. Superficial topography, profile measurements, and photography have been carried out using an optical confocal microscope (Sensofar Plμ2300, Nikon, Tokyo, Japan) and a stereoscope microscope. Absorbance spectrum and diffuse reflectance were measured using a double beam spectrophotometer UV-Vis-IR (Cary 500 Varian, Palo Alto, CA). Thermal trials and quality tests were performed at BSHE laboratories.

Results and Discussion

Laser Machining

The geometrical parameters obtained, that is, depth *Z*, width *A*, and removed volume *V*, depend on the optical properties of the laser beam, configuration

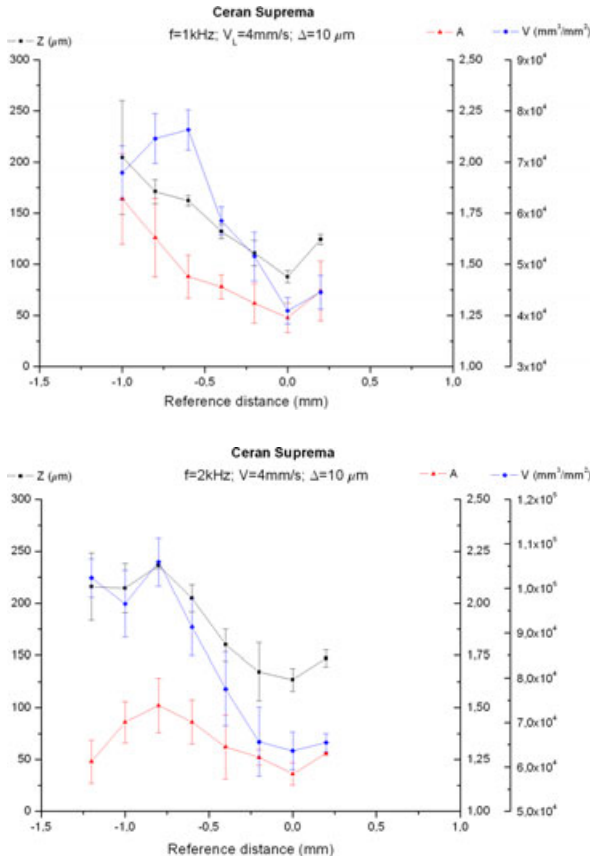

Fig. 2. Geometrical parameters obtained for 1 and 2 kHz.

of the laser system, working parameters, and mechanical, optical, and thermal properties of the substrate to be processed. In the first place, the substrate was machined in the surroundings of the focal point. Since the focal point is the place where the beam waist is minimal, the machined width will be minimal and the irradiance and the fluence reached will be maxima at this point. As Fig. 2 shows, the depth and the removed volume, like in the case of the machined width, are minimal in the vicinity of this point. The machined width has been expressed in percentage scale, referred to the 0.3 mm. Worth mentioning is that the volume and depth removed reach their maximum value out of focus. This behavior is independent of the substrate to be machined.[25] The reference distance where they are reached is around 500 and 700 μm below the focal plane for 1 and 2 kHz, respectively. As it is shown, a machined depth of up to 2.3 and 1.9 times higher and a removed volume of 1.8 and 1.6 times higher for 1

and 2 kHz, respectively can be obtained processing out of focus. Furthermore, another effect to take into account is the fact that the depth and the removed volume increase with the working frequency. In particular, at focus a depth of 88 and 127 μm with removed volumes of 4.1×10^4 and 6.36×10^4 mm^3/mm^2 can be obtained for 1 and 2 kHz, respectively.

In Fig. 3, the frontal views and profiles obtained machining at focus, (a), and -750 μm out of focus, (b), for 2 kHz are presented. As it is shown, in both cases the heat-affected zone, *HAZ*, is visible at first glance. This area is originated by the photothermal-mechanical character of the ablation process carried out by the NIR radiation. Furthermore, due to the fragile fracture nature of the glass-ceramic substrate, the edges of the machined areas are irregular and chipped. As Fig. 3b depicts, although the machined depth obtained processing out of focus is higher, as the focus is placed inside the substrate the edges of the groove are more irregular and chipped. This is because when the laser focus is placed slightly under the surface, the high power density of the laser beam originates a high pressure inside the material producing a micro-explosion, the shock wave of which is transferred to the nearby zones producing the ejection of the ceramic particles and the spallation of the material of the surface. As an example of how the micro-explosion is produced inside the material, Fig. 4 shows the inner imprints left by the laser beam when it is focused 0.5 mm under the surface. Both cases have been produced with laser pulses of 0.9 mJ, a peak power of 60 kW and a frequency of 2 kHz. In the first case, Fig. 4a, the laser beam has been scanned with a linear speed of 20 mm/s and in the Fig. 4b, the substrate has been irradiated with 50 pulses. In both cases, the imprint of the laser pulses and even the overlapping in the former show that the energy delivered onto the substrate is enough to modify the surface. However, although this amount of energy is not enough to overcome the threshold needed to machine the sample, the high pressure produced by the laser beam inside the material is such that some inner voids and cracks begin to appear under the surface. Hence, focusing inside the substrate enhances the ablation process. The focusing limit from which it is not possible to machine the samples is about 1 mm under the surface. For longer distances the pressure exerted inside the sample cannot be released toward the surface and produces the appearance of cracks in the whole sample and its rupture. The features of this kind of glass-ceramic substrates allow the NIR laser beam to be focused inside and, depending on the working conditions, permanent marks can be produced.[26] In the

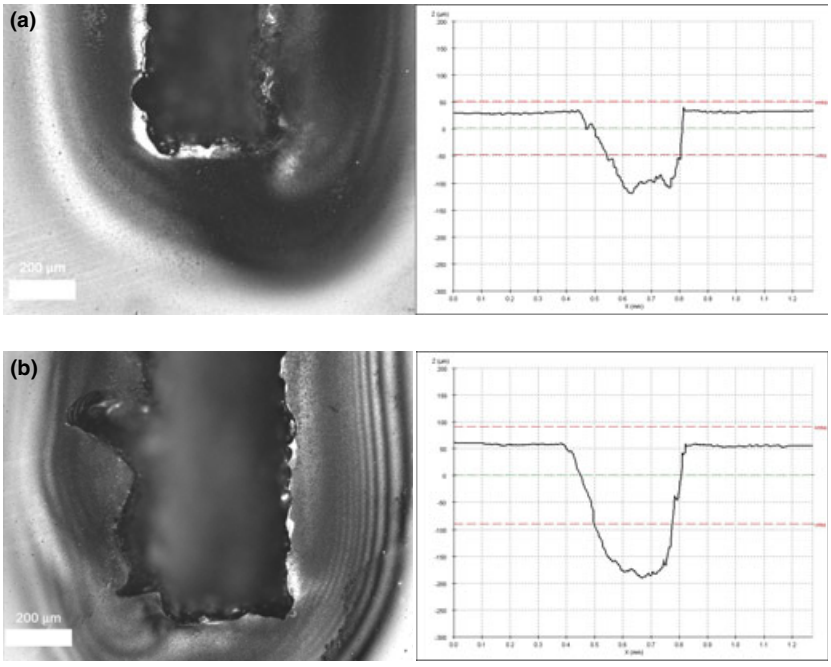

Fig. 3. Frontal view and profile of machining at focus, (a), and −750 μm out of focus, (b), for 2 kHz.

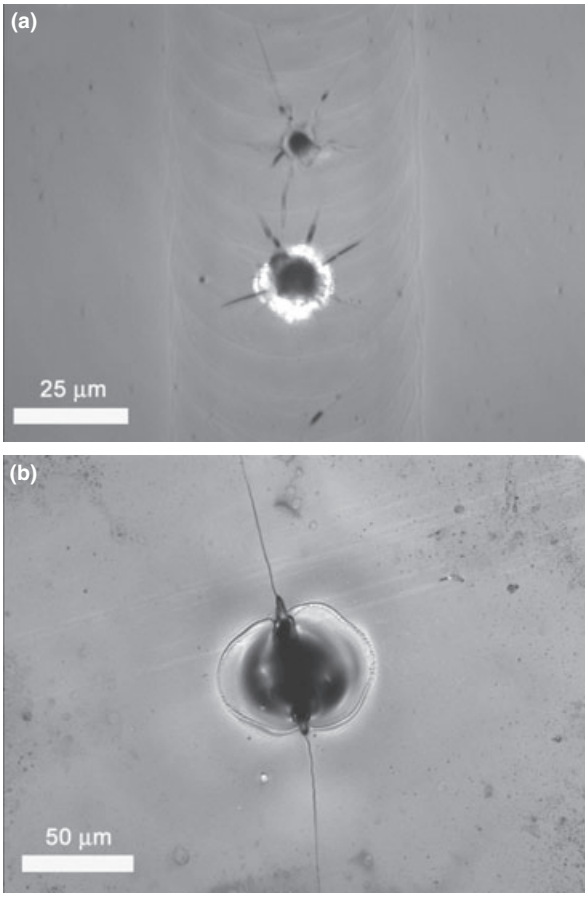

Fig. 4. Inner imprints left by the laser beam focusing 0.5 mm under the surface for laser pulses of 0.9 mJ, a peak power of 60 kW, a frequency of 2 kHz and scanning with a linear speed of 20 mm/s (a) and irradiating with 50 pulses (b).

case of transparent dielectric, the formation of nano-voids have been proven under femtosecond laser irradiation.[27,28]

To compare the ablation yield at the focal point and out of focus, the energy delivered per square millimeter was calculated by means of the pulse energy and the dynamic parameters of the process, that is, frequency, linear speed, and distance between adjacent lines and taking into account the removed volume per square millimeter at focus 4.1×10^4 and 6.36×10^4 mm^3/mm^2 and out of focus 7.6×10^4 and 1.06×10^5 mm^3/mm^2 for 1 and 2 kHz, respectively, resulting in an ablation yield of 0.11 and 0.13 J/cm^3 at focus and 0.06 and 0.08 J/cm^3 out of focus for 1 and 2 kHz, respectively. Therefore, as expected, the machining process is more efficient processing out of focus.

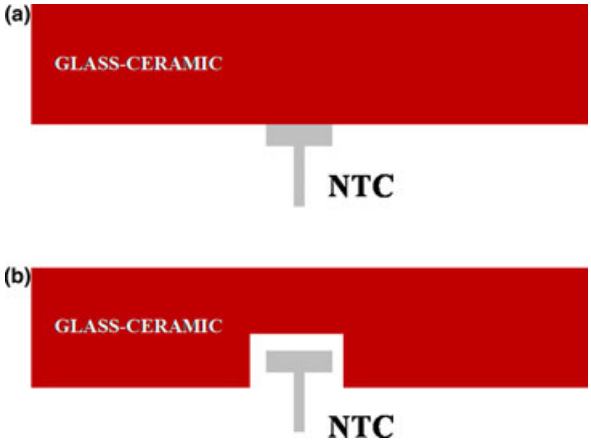

Fig. 5. Sketch of the negative temperature coefficient (NTC) electronic sensor placed at the classical position, (a), and new proposal, (b).

Functional Applications

Laser machining of blind holes in glass-ceramic sheets can be applied for inclusion of thermal sensors in the substrate and for fastening the glass-ceramic to other ceramic o metallic components.

Measurement of working temperature is of great importance in thermal processes. Energy cost reductions and efficiency improvement can generate more profitable methods. In this case, temperature is measured using Negative Temperature Coefficient (NTC) electronic sensors, placed at the lower surface of the glass ceramic sheet, Fig. 5a. Since the substrate is 4 mm thick, distance between lower and upper surfaces is too long to obtain values as accurate as was desirable. Thermal sensors can be approached to the upper surface drilling blind holes in the substrate, Fig. 5b. The response time for measuring the working temperature is optimized and more realistic values are obtained.[29]

The fastening of components to the glass-ceramic sheet is usually made by gluing, Fig. 6a. Since the sticking depends strongly on some parameters that are difficult to have under control, such as the glue's mixture or the ambient temperature, this procedure causes a lot of problems during the process, and in addition, gluing needs a drying stage. Therefore, time and a place where the samples can be stored are needed. One way

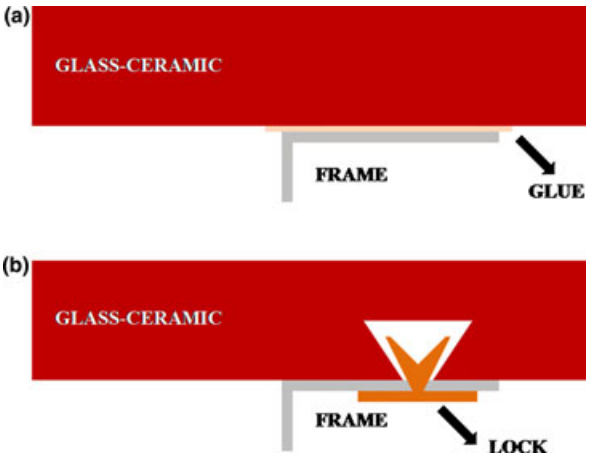

Fig. 6. Sketch of the sticking process for fastening the glass-ceramic to the metallic frame, (a), and new proposal, (b).

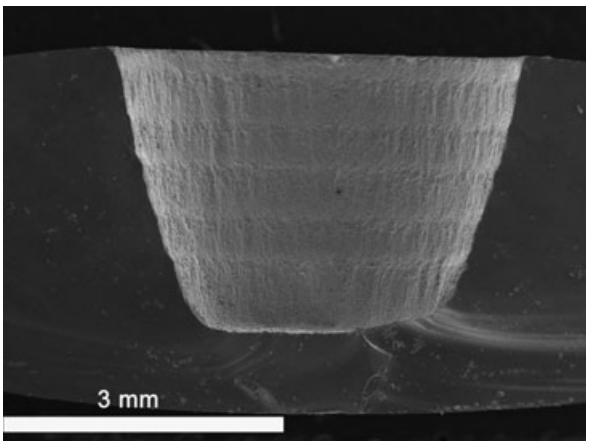

Fig. 7. Cross-section micrograph of the conical shape observed in the machining process.

of avoiding these problems is by machining special cross-section blind holes by laser and fastening the components directly to the glass-ceramic sheet, as is shown in Fig. 6b.[30]

To attain these objectives, blind holes of 2, 4, and 6 mm in diameter and 1, 2, and 3 mm in depth were machined. To achieve these depths the substrate was processed in cyclical stages, raising the substrate when the surface to be machined was out of the Rayleigh range. Beyond this range, the irradiance diminishes drastically and the efficacy of the process is not high enough to remove material from the surface.[1–3]

Figure 7 shows the cross-section micrograph of one of the resulting blind holes. Blind holes that are conical in shape are obtained by the tapering produced during the laser machining process. This tapering may be in relation to the linear polarization of the laser beam. Furthermore, six horizontal strips, which are related to the modification of the substrate position carried out during the processing, can be observed. On the other hand, the material ejected recasts over the upper surface, in the adjacent zones to the machined area, Fig. 8a, and over the walls and the bottom of the hole, Fig. 8b. Since the machined blind holes have to house thermal sensors the conical shape and the recast of material must be taken into account. The thermal transfer for the gathering of data depends on the roughness of the surface in contact with the sensor. To avoid the recast of material and to improve the roughness of the surface in contact with the sensor a gas jet has been injected during the process.

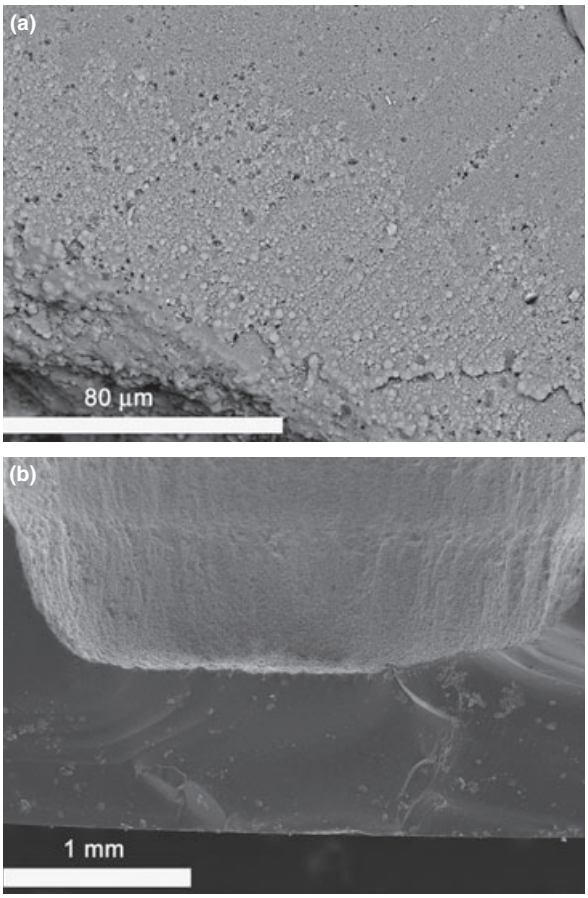

Fig. 8. Recast of material in the upper surface of the glass-ceramic sheet (a) and on the bottom and walls of the machined blind hole.

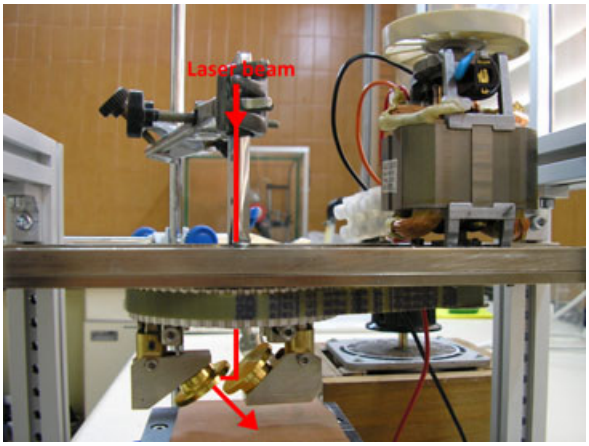

Fig. 9. Rotating system developed and coupled to the laser system to machine special cross-section blind hole.

To machine blind holes of any cross section, as Fig. 9 shows, a rotating system was developed and coupled to the laser system.[31] It consists of two mirrors, the position of which can be controlled to deflect the laser beam with the angle desired, attached to a rotating disk joined by a transmission belt to an engine of adjustable speed. These holes are machined in two stages. The first one is to machine a blind hole by the standard method and afterward the rotating system is coupled for removing the material from the lateral sides. By adjusting the tilt of the mirrors the incidence angle of the laser could be controlled and any shape can be obtained as it is shown in the cross section of Fig. 10.

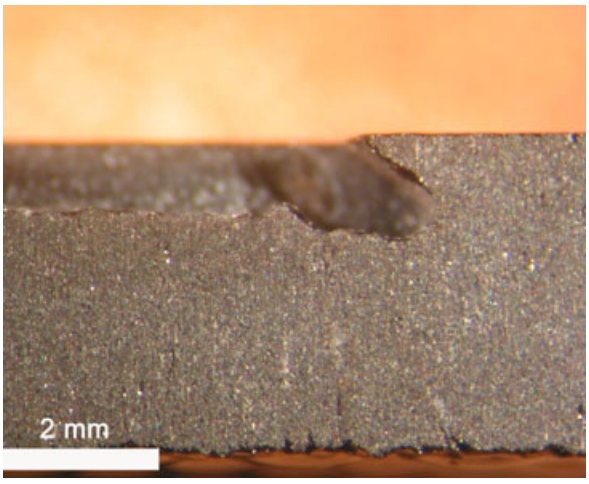

Fig. 10. Cross-section view of a blind hole obtained by varying the incidence angle.

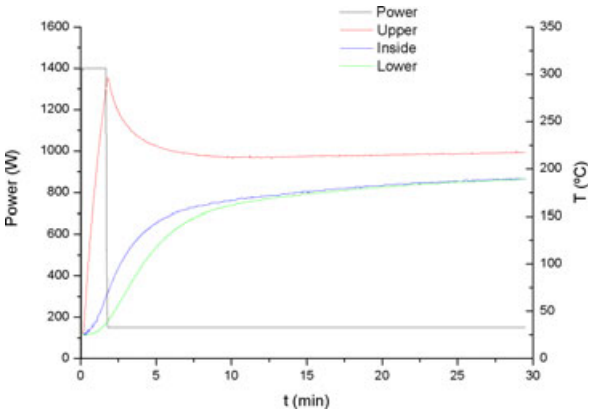

Fig. 11. Temperature values obtained comparing sensors in the lower surface and inside a blind hole machined compared with respect to the temperature of the upper surface.

The elemental composition of the heat-affected zone was analyzed by using semiquantitative EDS microanalysis, concluding that there is no variation in the composition of the glass-ceramic sheet. In the same way, the mechanical properties were characterized in these areas and compared to the former by Vickers microhardness, observing a decrease of about a 20% in the *HAZ*. Finally, the working temperature was measured by comparing sensors in the lower surface and inside a blind hole machined in the glass sheet with respect to the temperature of the upper surface. As Fig. 11 depicts, the values obtained by the sensor inside the substrate are closer to real temperatures and are acquired in shorter times.

Conclusions

A NIR Q-Switch laser system was used to study the glass-ceramic laser machining and some functional applications have been proposed. The effect produced by the machining method and how the modification in the reference position influences the morphology of the geometrical parameters and the ablation yield have been shown, obtaining that the maximal depth and volume are obtained when the surface to be machined is placed out of focus in such a way that the machining process is more efficient processing out of focus. Furthermore, it has been shown how, when the laser focus is placed slightly under the surface, a micro-explosion is originated the shock wave of which is transferred to the nearby zones, producing the ejection of the ceramic

particles and the spallation of the material of the surface enhancing the ablation process.

Laser machining has been applied for inclusion of thermal sensors in the substrate and for fastening purposes. The glass-ceramic was drilled reducing the distance between working temperature and thermal sensor, diminishing the response time, and obtaining more accurate values.

Blind holes of any cross section were machined coupling an additional rotating system, in such a way that they can be used to fasten metallic or ceramic components to the glass sheet, avoiding sticking processes. Modifications of mechanical properties in the machined zone and in adjacent areas were studied finding no substantial variations compared to the substrate without processing.

Acknowledgments

Daniel Sola thanks the JAE-DOC program, BSH Home Appliances Group and the Science and Technology Inter-Ministry commission of Spain and FEDER funds of the EC under project MAT2009-13979-C03-03 for the financial support of his contract.

References

1. W. Steen, *Laser Material Processing*, Springer-Verlag, Heidelberg, Germany, 1999.
2. D. Bäuerle, *Laser Processing and Chemistry*, Springer-Verlag, Heidelberg, Germany, 2000.
3. M. Allmen and A. Blatter, *Laser-Beam Interactions with Materials*, Springer-Verlag, Heidelberg, Germany, 1995.
4. Y. Pauleau, *Materials Surface Processing by Directed Energy Techniques*, Elsevier, Oxford, U.K., 2006.
5. H. Misawa and S. Juodkazis, *3D Laser Microfabrication*, John Wiley and Sons, Weinheim, Germany, 2006.
6. E. G. Gamaly, A. V. Rode, and B. Luther-Davies, "Ultrafast Ablation with High-Pulse-Rate Lasers. Part I: Theoretical Considerations," *J. Appl. Phys.*, 85 4213–4221 (1999).
7. A. V. Rode, B. Luther-Davies, and E. G. Gamaly, "Ultrafast Ablation with High-Pulse-Rate Lasers. Part II: Experiments on Laser Deposition of Amorphous Carbon Films," *J. Appl. Phys.*, 85 4222–4230 (1999).
8. N. M. Bulgakova and A. V. Bulgakov, "Pulsed Laser Ablation of Solids: Transition from Normal Vaporization to Phase Explosion," *Appl. Phys. A*, 73 199–208 (2001).
9. M. A. Anisimov, "Investigation of Critical Phenomena in Liquids," *Sov. Phys.-Usp*, 17 249–294 (1975).
10. B. N. Chichkov, C. Momma, S. Nolte, F. Von Alvensleben, and A. Tünnermann, "Femtosecond, Picoseconds and Nanosecond Laser Ablation of Solids," *Appl. Phys. A*, 63 109–115 (1996).
11. C. Momma, *et al.* "Short Pulse Laser Ablation of Solid Targets," *Opt. Commun.*, 129 134–142 (1996).
12. A. V. Bulgakov and N. M. Bulgakova, "Thermal Model of Pulsed Laser Ablation Under the Conditions of Formation and Heating of a Radiation-Absorbing Plasma," *Quant. Elec.*, 29 433–437 (1999).
13. A. Gusarov and I. Smurov, "Thermal Model of Nanosecond Pulsed Laser Ablation: Analysis of Energy and Mass Transfer," *J. Appl. Phys.*, 97 014307 (2005).
14. R. K. Singh and J. Narayan, "Pulsed Laser Evaporation Technique for Deposition of Thin Films-Physics and Theoretical Model," *Phys. Rev. B*, 41 8843–8859 (1990).
15. S. Amoruso, R. Bruzzese, N. Spinelli, and R. Velotta, "Characterization of Laser-Ablation Plasmas," *J. Phys. B: At. Mol. Opt. Phys.*, 32 R131–R172 (1999).
16. P. R. Willmott and J. R. Huber, "Pulsed Laser Vaporization and Deposition," *Rev. Mod. Phys.*, 72 315–328 (2000).
17. M. Tode, Y. Takigawa, and M. Masato, "Hot-Target Laser Ablation is Critical for Beta-FeSi2 Growth on Si without Fragments," *Met. Mat. Trans. A*, 39 A 130–A 134 (2008).
18. A. Braun, K. Zimmer, and F. Bigl, "Combination of Contour and Half-Tone Masks used in Laser Ablation," *Appl. Surf. Sci.*, 168 178–181 (2000).
19. J. H. Kim, S. Lee, and H. S. Im, "The Effect of Different Ambient Gases, Pressures, and Substrate Temperatures on TiO2 Thin Films Grown on Si (100) by Laser Ablation Technique," *Appl. Phys. A*, 69 S629–S632 (1999).
20. J. A. Pardo, J. I. Peña, R. I. Merino, R. Cases, A. Larrea, and V. M. Orera, "Spectroscopic Properties of Er^{3+} and Nd^{3+} Doped Glasses with the $0.8CaSiO_3$–$0.2Ca_3(PO_4)_2$ Eutectic Composition," *J. Non-Cryst. Solids*, 298 23–31 (2002).
21. R. Balda, R. I. Merino, J. I. Peña, V. M. Orera, and J. Fernández, "Laser Spectroscopic of Nd^{3+} Ion Glasses with the $0.8CaSiO_3$–$0.2Ca_3(PO_4)_2$ Eutectic Composition," *Opt. Mater.*, 31 1319–1322 (2009).
22. R. Balda, R. I. Merino, J. I. Peña, V. M. Orera, M. A. Arriandiaga, and J. Fernández, "Spectroscopic Properties and Frequency Upconversion of Er^{3+} Doped the $0.8CaSiO_3$–$0.2Ca_3(PO_4)_2$ Eutectic Glass," *Opt. Mater.*, 31 1105–1108 (2009).
23. R. Balda, *et al.* "Broadband Laser Tunability of Nd^{3+} Ions in $0.8CaSiO_3$–$0.2Ca_3(PO_4)_2$ Eutectic Glass," *Optics Express*, 17 4382–4387 (2009).
24. R. Balda, J. I. Peña, M. A. Arriandiaga, and J. Fernández, "Efficient $Nd^{3+} \rightarrow Yb^{3+}$ Energy Transfer in $0.8CaSiO_3$–$0.2Ca_3(PO_4)_2$ Eutectic Glass," *Opt. Exp.*, 18 13842–13850 (2010).
25. D. Sola, A. Escartin, R. Cases, and J. I. Peña, "Laser Ablation of Advanced Ceramics and Glass-Ceramic Materials: Reference Position Dependence," *Appl. Surf. Sci.*, 257 5413–5419 (2011).
26. D. Sola, A. Escartin, R. Cases, and J. I. Peña, "Crystal Growth Induced by Nd:YAG Laser Irradiation in Patterning Glass Ceramic Substrates with Dots," *Opt. Mater.*, 33 728–734 (2011).
27. E. G. Gamaly, *et al.* "Formation of Nano-Voids in Transparent Dielectrics by Femtosecond Lasers," *Curr. Appl. Phys.*, 8 412–415 (2008).
28. S. Juodkazis, H. Misawa, T. Hashimoto, E. G. Gamaly, and B. Luther-Davies, "Laser-Induced Microexplosion Confined in a Bulk of Silica: Formation of Nanovoids", *Appl. Phys. Lett.* 88 201909-1–201909-3 (2006).
29. M. A. Buñuel, J. Ceamanos, J. R. García, R. I. Merino, J. I. Peña, and D. Sola, "Campo de cocción con una zona de sensor de temperatura," Spanish Patent P200700755, 2007.
30. M. A. Buñuel, *et al.* "Campo de cocción con una placa de cubierta y un elemento de montaje," European Patent P200703062, 2007.
31. I. Asensio, M. A. Buñuel, J. R. García, J. I. Peña, and D. Sola. "Abdeckplatte aus Glas oder Keramik für ein Hausgerät und Verfahren zum Herstellen einer Abdeckplatte," German Patent DE102008043456, 2008.